Geometric Modeling and Global Optimization for Plant Line Identification in Agricultural Orthomosaics

Willian Moreira Antunes*1, Bruno Moraes Rocha*2, Emilia Alves Nogueira*3,
Juliana Paula Felix*4, Fabrizzio Soares*5
*Federal University of Goiás, Pixelab Laboratory, Goiânia, GO, Brazil
1willianantunes@discente.ufg.br, 2rocha3runo@gmail.com, 3emiliacdc8@gmail.com,
4jufelix16@gmail.com, 5Fabrizzio.soares@gmail.com

***Abstract*—Accurate detection of planting lines in high-resolution orthomosaics is a prerequisite for many precision agriculture applications, yet existing methods struggle with field-specific challenges such as vegetation gaps, segmentation artifacts, and partial occlusions. We propose a hybrid pipeline that first segments crop rows by exploiting the HSV color space and a lightweight K-Nearest Neighbors (KNN) classifier, followed by morphological refinement to suppress noise.The resulting binary mask is then interpreted as a set of parallel lines whose orientation, spacing, and offset are jointly optimized in a global parametric framework. A compound cost function—penalizing deviations from the mask, penalizing large residuals, and encouraging uniform spacing—is minimized using Differential Evolution, a population-based optimization algorithm that is robust to local minima. Because the method relies only on generic color cues and a simple line model, it does not require large annotated datasets. Experiments on a diverse set of crop fields show that our approach achieves line coverage exceeding 95%, with high accuracy and improved performance over segmentation-only approaches in challenging scenarios. These results demonstrate that the proposed technique is well suited for autonomous navigation, gap detection, and other downstream tasks in precision agriculture.**

***Index Terms*—Differential evolution, Combinatorial optimization, Real-world applications, Intelligent Agriculture.**

I. Introduction

Precision agriculture has become essential for enhancing productivity and sustainability in crop management, largely supported by integrating remote sensing, high-resolution aerial imagery, and image analysis algorithms. In particular, the automatic identification of planting lines in orthomosaics acquired by Unmanned Aerial Vehicles (UAVs) is crucial for applications such as autonomous machine navigation, seeding gap detection, and spatial monitoring of crop development [1].

Despite the potential of orthomosaics, robust planting line detection faces significant practical challenges—including illumination variations, exposed soil, shadows, weed presence, and vegetation discontinuities—that can degrade the performance of classical geometric methods based on the Hough Transform. Recent studies show that although Hough and its variants remain useful, they can be unstable in areas with extensive non-vegetated regions or partially curved lines, often requiring complementary pre-processing and post-processing strategies [2]. Moreover, traditional methods typically rely on handcrafted features and manually tuned thresholds, which may not generalize well under varying environmental conditions [3].

Recent advances in deep learning have introduced more robust solutions, such as Vision Transformers (ViTs) and hybrid CNN-ViT architectures, which excel in capturing global contextual information and long-range dependencies essential for accurate crop row segmentation under complex field conditions [3]. For instance, architectures like ConvFormer and CAFormer have demonstrated superior performance in segmentation tasks by integrating convolutional inductive biases with self-attention mechanisms, achieving high precision and recall even in challenging agricultural scenes [3]. However, these deep learning approaches often demand substantial annotated datasets and significant computational resources, limiting their applicability in scenarios with limited data or real-time constraints.

Literature on vegetation segmentation indicates that, in agricultural scenarios with spectral variation and limited annotated data, lightweight approaches based on color spaces (e.g., HSV) combined with simple classifiers (e.g., KNN) remain relevant due to their simplicity and computational efficiency [4]. Reviews on segmentation and microplots also emphasize the usefulness of multiscale features and combined color spaces to increase robustness [4].

As an alternative to purely Hough-based methods or end-to-end deep learning solutions—which often demand large annotation volumes and higher computational cost—hybrid approaches that unite efficient segmentation with explicit geometric modeling offer a balance between robustness, interpretability, and cost. Furthermore, formulating line estimation as a global optimization problem allows efficient exploration of non-convex parameter spaces and reduces sensitivity to local minima. Previous works adopting global formulations or energy minimization provide the theoretical basis for this choice [5].

Recent works have demonstrated that convolutional neural networks (CNNs) are particularly effective for segmenting crop lines from UAV imagery, even in the presence of noise and varying crop conditions [6]. For instance, U-Net, LinkNet, and PSPNet architectures have been successfully applied to sugarcane plantations, achieving high Dice coefficients and robust performance across diverse datasets [6]. These networks benefit from transfer learning with pre-trained encoders, such as VGG16, to extract discriminative features, yet their ability to generalize across different crop phases (e.g., plant vs. ratoon) remains a challenge [6]. Furthermore, while deep learning methods provide strong segmentation, they often require large labeled datasets and significant computational resources, which may not be feasible in all operational contexts.

In this context, we propose a hybrid method that differs from classical line detection pipelines. More specifically, this work introduces a global parametric formulation for crop row detection, in which orientation, spacing, and offset are jointly estimated as a coupled geometric structure. A compound cost function is designed to integrate geometric alignment, false-positive penalization, spacing regularization, and angular diversity, enabling robust recovery even under fragmented vegetation and segmentation artefacts.

II. Related Work

The automatic detection of planting lines in aerial and ground images is a central theme in precision agriculture, as it supports machine navigation, gap mapping, and crop monitoring [7].

A. Vegetation Segmentation and Extraction

Separating vegetation from background (soil/shadow/straw) is often addressed by thresholding vegetation indices or by classifiers in color spaces. In agricultural environments with illumination and texture variations, methods based on multiscale attributes and multiple color spaces (including HSV and $L^*a^*b^*$) have been explored to improve segmentation robustness, especially when spectral contrast is low [8]. Recent reviews show that, despite advances in deep networks, traditional and low-cost supervised approaches (e.g., using color spaces and lightweight classifiers) remain relevant in scenarios with few annotated data and need for practical implementations [9], [10].

B. Geometric Detection of Planting Lines

After segmentation, classical approaches model planting lines as dominant straight lines and apply variants of the Hough Transform, often combined with pre-processing (edges, clustering, filtering) to stabilize detection in the presence of noise and gaps [11]–[13]. A body of work in UAV imagery reinforces that Hough-based methods have historically been common but can be unstable when lines are discontinuous, partially curved, or when large non-vegetated regions are present [2].

C. Deep Learning Approaches

More recently, deep learning techniques have been employed for end-to-end segmentation and/or detection of lines, improving performance under complex conditions. Models combining CNNs with geometric priors and/or line detection stages have been proposed for UAV images, seeking robustness to field variations [14]. There are also end-to-end proposals that treat each line as an object and reduce dependence on post-processing, with gains in generality [15]. Moreover, lightweight segmentation networks for navigation line extraction have been investigated for real-time applications [16]. However, deep methods often require representative annotated datasets and higher computational cost, motivating hybrid and alternative solutions with lower labeling needs [17].

D. Global Optimization and Parametric Modeling

In this context, global optimization meta-heuristics are attractive for exploring non-convex spaces and reducing sensitivity to local minima. In particular, *Differential Evolution* (DE) is a classical and widely used method for global continuous optimization [18].

Unlike purely Hough-based approaches or end-to-end deep solutions, this work adopts a hybrid strategy: segmentation using *KNN* in HSV with morphological refinement, followed by fitting a parametric model of parallel lines via *DE*, allowing robustness to gaps/discontinuities and reducing dependence on large volumes of annotated data.

III. Proposed Method

A. Study Region and Orthomosaic

This study utilizes the same dataset of RGB aerial imagery described by Rocha et al. [19], originally captured for the detection and evaluation of gaps in curved sugarcane planting lines. The images were acquired in the rural region of Quirinópolis, Goiás, Brazil, using a BATMAP I UAV equipped with a Sony Alpha 6000 RGB camera. Flights were conducted at an altitude of 200 m, ensuring high spatial detail suitable for agricultural inspection.

Following the methodology outlined in [19], the imagery was georeferenced using Ground Control Points (GCPs) surveyed with an RTK-GNSS system (Spectra Precision SP60). The images were then processed into georeferenced orthomosaics in GeoTIFF format, with a spatial resolution of approximately 0.5 m per pixel. This resolution allows clear discrimination of planting rows and inter-row gaps, which is essential for precise gap detection.

The dataset includes images from two key growth stages of sugarcane: 40 and 80 days after harvest (DAH). These stages were selected because the crop canopy is sufficiently developed to cover the rows while still leaving inter-row spaces visible, facilitating accurate gap identification [19]. The scenes also exhibit a variety of agricultural features—such as curved and straight planting lines, terraces, unpaved roads, trees, and shadows—providing a realistic and challenging testbed for evaluating the robustness of the proposed processing pipeline.

To facilitate supervised evaluation and validation, it was necessary to manually annotate specific sugarcane field plots within the orthomosaics. This manual delineation was performed using QGIS software, following the same annotation protocol described in [19], and served as ground truth for training and testing the detection models.

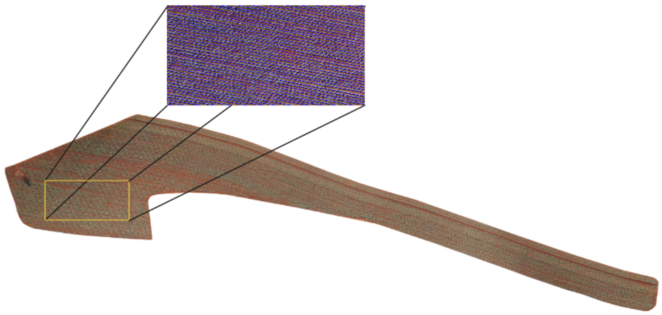

Fig 1: Example of manually marked planting lines

B. Orthomosaic Processing and Tiling

The orthomosaic was loaded and processed using the *Rasterio* library, represented as a three-dimensional array in the format (b, h, w), where b denotes the number of spectral bands (R, G, B). To facilitate computationally efficient analysis and to handle curved crop rows more effectively, the orthomosaic was divided into regular, non-overlapping blocks (tiles) of 256×256 pixels, following a block-partitioning strategy similar to that adopted by Rocha et al. [19]. Each tile was treated as an independent processing unit, enabling parallel computation and reducing memory overhead while preserving local geometric features of the planting rows.

C. HSV Color Space Transformation and KNN-Based Vegetation Segmentation

To enhance the separability between vegetation and background elements such as soil and shadows, each RGB tile was transformed into the HSV color space. The HSV representation decouples chromatic information from illumination, making it more suitable for vegetation discrimination in aerial imagery.

Instead of using the full HSV vector, only the Hue (H) and Saturation (S) components were employed, as they contain the most discriminative information for vegetation detection. The Value (V) channel was intentionally discarded to reduce sensitivity to illumination variations and shadow effects.

Let $\mathbf{x}_i = (H_i, S_i)$ be the feature vector of a pixel in the HSV space. These components were physically normalized according to their natural ranges:

$$H_i' = \frac{H_i}{180}, \qquad S_i' = \frac{S_i}{255} \tag{1}$$

A *K-Nearest Neighbors* (KNN) classifier was trained using manually selected HSV samples representing two classes: sugarcane vegetation and non-vegetation (soil and shadow). The classifier employed Euclidean distance with distance-based weighting.

After training, each pixel of the tile was classified individually using the normalized (H', S') features, resulting in a binary vegetation mask defined as:

$$I(x, y) = \begin{cases} 1, & \text{vegetation pixel} \\ 0, & \text{non-vegetation pixel} \end{cases} \tag{2}$$

To reduce noise and remove small spurious regions, the binary mask was further refined using morphological closing and opening operations followed by connected component filtering.

D. Morphologic Post-Processing

The initial binary mask contains noise due to local spectral variations. To correct this, sequential morphological operations were applied:

- Closing:for gap filling;
- Opening: for isolated noise removal.

An elliptical structuring element of size 3×3 pixels was used. Subsequently, connected components with an area smaller than a minimum threshold were removed, resulting in a clean final vegetation mask.

E. Parametric Modeling of Crop Lines

The planting rows were modeled as a set of parallel lines described by the parameter vector:

$$\mathbf{p} = \{\theta, s, o\} \tag{3}$$

where:

- $\theta \in [0°, 180°]$ is the orientation angle;
- s is the mean line spacing;
- o is the *offset*.

From these parameters, a synthetic mask $M(\mathbf{p})$ containing parallel lines with fixed thickness is generated.

F. Cost Function

The estimation of the parameters $\mathbf{p}$ was formulated as an optimization problem that minimizes a cost function $J(\mathbf{p})$, computed from the vegetation mask I and a synthetic line mask.

Unlike classical formulations that evaluate only the current line hypothesis, the proposed method evaluates the union between the current line set and previously detected line sets. This strategy allows incremental recovery of multiple line families while preventing redundant detections.

Let $M(\mathbf{p})$ be the synthetic mask generated from the current parameters and, if available, let $M(\mathbf{p}')$ be the mask associated with a previously accepted solution. The effective mask used in the cost evaluation is defined as:

$$M_{tot} = \max\left(M(\mathbf{p}),\ M(\mathbf{p}')\right) \tag{4}$$

If no previous solution exists, then $M_{tot} = M(\mathbf{p})$.

1) Mean Distance to Lines: First, the Euclidean distance map to the nearest synthetic line is computed:

$$D = EDT(M_{tot} = 0) \tag{5}$$

The distance cost is defined as:

$$J_d = \frac{1}{|I|} \sum_{(x,y) \in I=1} \frac{D(x, y)}{n} \tag{6}$$

where n is the tile size.

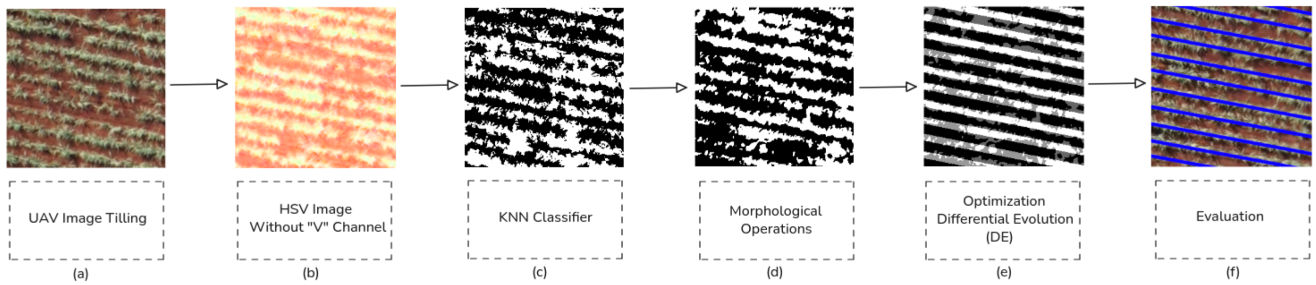

Fig 2: Overview of the proposed pipeline for automatic planting line identification in agricultural orthomosaics. (a) UAV orthomosaic divided into 256256 tiles; (b) conversion to HSV color space using only Hue and Saturation components; (c) pixel-wise vegetation segmentation using a KNN classifier; (d) morphological closing and opening with small component removal to obtain a clean binary vegetation mask; (e) geometric modeling of crop rows as parallel lines whose parameters are optimized via Differential Evolution using a distance-based cost function; and (f) final detected crop lines overlaid on the original tile for evaluation and downstream agricultural applications, highlighting the integration between segmentation and global geometric optimization.

2) Penalty for False Positives: To avoid placing lines over non-vegetated regions:

$$J_{fp} = \frac{|M_{tot} \cap (I = 0)|}{|M_{tot}|} \tag{7}$$

3) Spacing Regularization: The spacing is weakly regularized around a scale-aware reference value derived from the image size. This reference does not impose a fixed inter-row distance but stabilizes the optimization search by reflecting the typical proportion between row spacing and tile dimensions observed in agricultural orthomosaics.

This term acts as a soft constraint rather than enforcing a fixed spacing value, allowing the model to adapt to natural variations in planting patterns.

$$s_{opt} = \frac{n}{12} \tag{8}$$

$$J_s = \left(\frac{s - s_{opt}}{s_{opt}} \right)^2 \tag{9}$$

If a previous solution exists, the same regularization term is also applied to the spacing associated with that solution.

4) Angular Diversity Penalty: To prevent the optimizer from repeatedly detecting the same line orientation, the angular difference between the current and previous solution is evaluated:

$$\Delta\theta = \min(|\theta - \theta'|,\ 180^\circ - |\theta - \theta'|) \tag{10}$$

If $\Delta\theta < 30^\circ$, a penalty J_θ is added.

5) Final Cost Function: The complete cost function combines geometric alignment, false positive suppression, spacing regularization, and angular diversity into a single objective:

$$J(\mathbf{p}) = J_d + \lambda_{fp} J_{fp} + \lambda_s J_s + \lambda_\theta J_\theta \tag{11}$$

The weights were tuned on a validation set to prioritize geometric alignment while adequately regularizing spacing and angular diversity. The final values ($\lambda_{fp} = 0.2$, $\lambda_s = 0.02$, $\lambda_\theta = 0.5$) reflect this balance, with J_d dominating the cost function to ensure accurate line fitting.

Algorithm 1 Cost Function $J(\mathbf{p})$

Require: Binary vegetation mask I, parameters $\mathbf{p} = \{\theta_1, s_1, o_1\}$, previous best $\mathbf{p}'$ (optional)
Ensure: Cost $J(\mathbf{p})$
$n \leftarrow$ image size
$s_{min} \leftarrow 4, \quad s_{max} \leftarrow n/4$
$s_1 \leftarrow \text{clip}(s_1, s_{min}, s_{max})$
$M_1 \leftarrow \text{GenerateLinesMask}(n, \theta_1, s_1, o_1)$
$M_2 \leftarrow 0$
if $\mathbf{p}'$ exists **then**
  $(\theta_2, s_2, o_2) \leftarrow \mathbf{p}'[0:3]$
  $s_2 \leftarrow \text{clip}(s_2, s_{min}, s_{max})$
  $M_2 \leftarrow \text{GenerateLinesMask}(n, \theta_2, s_2, o_2)$
end if
$M_{tot} \leftarrow \max(M_1, M_2)$
if $\sum_{x,y} M_{tot}(x, y) = 0$ **then**
  return 10^6
end if
$D \leftarrow \text{EDT}(M_{tot} = 0)$
$d_{mean} \leftarrow \text{mean}\big(D(x, y) \mid I(x, y) > 0\big)/n$
$J \leftarrow d_{mean}$
$fp \leftarrow |(I = 0) \cap M_{tot}|$
$fp\_rate \leftarrow \dfrac{fp}{|M_{tot}| + 10^{-6}}$
$J \leftarrow J + 0.2 \cdot fp\_rate$
$s_{opt} \leftarrow n/12$
$J \leftarrow J + 0.02 \left(\dfrac{s_1 - s_{opt}}{s_{opt}} \right)^2$
if $\mathbf{p}'$ exists **then**
  $J \leftarrow J + 0.02 \left(\dfrac{s_2 - s_{opt}}{s_{opt}} \right)^2$
end if
if $\mathbf{p}'$ exists **then**
  $\Delta\theta \leftarrow |\theta_1 - \theta_2|$
  $\Delta\theta \leftarrow \min(\Delta\theta,\ 180^\circ - \Delta\theta)$
  if $\Delta\theta < 30^\circ$ **then**
    $J \leftarrow J + 0.5$
  end if
end if
return J

Algorithm 2 Identifying Lines Mask

Require: Image size n, angle θ, spacing s, offset o
Ensure: Binary mask M containing parallel lines

Initialize $M \leftarrow 0_{n \times n}$
$\theta_r \leftarrow \theta \cdot \pi/180$
Direction vector: $(d_x, d_y) \leftarrow (\cos\theta_r, \sin\theta_r)$
Normal vector: $(n_x, n_y) \leftarrow (-d_y, d_x)$
$c \leftarrow n/2$
$k_{max} \leftarrow n/s + 2$
for $k = -k_{max}$ to k_{max} **do**
  $l \leftarrow o + k \cdot s$
  $P_1 \leftarrow (c - nd_x + ln_x,\ c - nd_y + ln_y)$
  $P_2 \leftarrow (c + nd_x + ln_x,\ c + nd_y + ln_y)$
  Draw line P_1P_2 on M
end for
return M

G. Optimization Settings

The optimization problem defined in Eq. (11) is solved using Differential Evolution (DE) with the "best1bin" strategy. The population size was set to 55, and the algorithm was executed for 150 generations. The mutation factor was defined in the range $F \in [0.5, 1.0]$, and the crossover rate was set to $CR = 0.7$. The parameter bounds were defined as $\theta \in [0°, 180°]$, $s \in [10, n]$, and $o \in [-100, 100]$, where n denotes the tile size. A final polishing step was applied, and parallel evaluation was used to improve computational efficiency.

IV. Results and Discussion

A. Experimental Setup and Evaluation Metrics

The proposed method was evaluated on a total of 95 image tiles (256×256 pixels) extracted from sugarcane orthomosaics, covering both growth stages (40 and 80 days after harvest). Selected tiles represent diverse field conditions, including variations in illumination, vegetation density, soil exposure, and partial occlusions. Four geometry-aware metrics were employed to quantify the structural alignment between detected and reference lines:

- **Mean Distance Error (MDE)**: Average Euclidean distance [px] between vegetation pixels and the nearest detected line, normalized by image size.
- **Line Coverage Rate**: Proportion of ground truth line pixels that lie within a tolerance radius (1 px) of any detected line.
- **Angular Error**: Absolute difference [deg] between the estimated orientation θ and the ground truth dominant angle.
- **Spacing Error**: Absolute deviation [px] between the estimated inter-row spacing s and the reference spacing measured from annotations.

B. Quantitative Performance Analysis

Table I summarizes the quantitative results aggregated over all test blocks. The proposed method achieved high accuracy in recovering the geometric structure of planting lines.

TABLE I
Geometric Evaluation Results for Planting Line Detection

Metric	Mean	Std. Dev.	Min	Max
Mean Distance Error (MDE) [px]	0.2250	0.2489	0.0441	1.2823
Line Coverage Rate	0.9810	0.0610	0.7601	0.9850
Angular Error [deg]	1.3350	4.5210	0.0150	21.5130
Spacing Error [px]	3.3710	2.3320	0.0010	7.4960

1) Alignment Accuracy (MDE and Coverage): The low Mean Distance Error (0.225 px on average) demonstrates precise geometric alignment between detected lines and vegetation patterns. This sub-pixel accuracy confirms the effectiveness of the global optimization framework in fitting the parametric model to irregular vegetation distributions. The high Line Coverage Rate (98.1%) indicates that the method successfully captures the majority of planting line structure, with performance degradation occurring only in blocks with extensive vegetation gaps exceeding 40% of row length.

2) Orientation and Spacing Recovery: Average Angular Error of 1.335, with a maximum deviation of 21.513, indicating that the method generally achieves great orientation estimation, although occasional larger deviations occur in more challenging scenarios. Average Spacing Error of 3.371 px, mainly influenced by inherent planting irregularities and the regularization term based on s_{opt}. This value does not enforce a fixed spacing; instead, it serves as a scale-aware reference proportional to tile size, helping to stabilize the optimization process in agricultural orthomosaics.

C. Visual Results and Qualitative Assessment

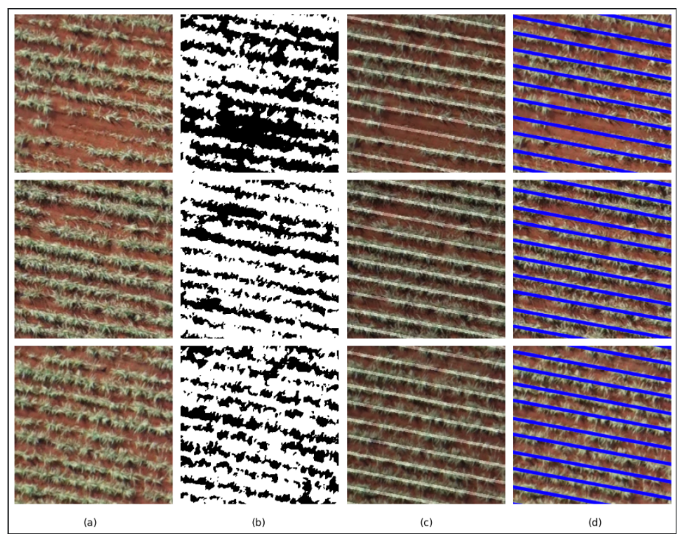

Fig 3: Results of the vegetation row detection methodology. (a) Original crop block image; (b) Initial vegetation segmentation via KNN classifier; (c) Predicted mask with Differential Evolution (DE) algorithm; (d) Reference ground truth mask for accuracy assessment.

Figure IV-C illustrates detection result on a representative block with continuous vegetation. Parametric model successfully aligns lines precisely with underlying crop rows, despite presence of minor gaps in vegetation. This demonstrates robustness of the global optimization approach in maintaining row structure even when local features are incomplete.

D. Comparative Advantages and Limitations

Classical Hough and RANSAC-based methods typically produce fragmented detections or incorrect orientations when vegetation gaps exceed 30–40% of row length, due to their reliance on local evidence. In contrast, the proposed global formulation remains stable due to entire line family is optimized simultaneously from distributed vegetation evidence. Tiling is adopted primarily for computational efficiency, also parametric formulation itself is not restricted to block processing.

E. Practical Implications for Precision Agriculture

The achieved accuracy levels directly support key precision agriculture applications. The sub-pixel line alignment enables reliable autonomous guidance for machinery, while the robust gap detection (visualized as line segments without underlying vegetation) facilitates targeted replanting interventions. The method's consistency across varying vegetation conditions makes it suitable for large-scale monitoring operations without requiring per-field parameter tuning.

V. Conclusion and Future Work

This work introduced a global parametric formulation for crop-row structure recovery from noisy vegetation masks in UAV orthomosaics. By modeling planting rows as a coupled geometric structure rather than independent lines, the proposed method overcomes limitations of classical Hough/RANSAC-based detectors and avoids data requirements of deep learning.

The results demonstrate that the proposed method reliably recovers planting line structures even in the presence of vegetation gaps, segmentation noise, and partial occlusions. Quantitative evaluation using geometry-aware metrics—such as Mean Distance Error, Line Coverage Rate, Angular Error, and Spacing Error—confirmed the robustness and accuracy of the proposed solution, with low error values and high coverage rates across the evaluated image blocks.

These results highlight the effectiveness of global geometric optimization as a practical alternative to both local detection methods and data-intensive learning-based approaches in precision agriculture. Overall, the proposed method provides a robust, interpretable, and computationally efficient solution for crop row detection in real-world agricultural scenarios.

A. Future Work

Future work considers extending parametric formulation to handle curved planting patterns, incorporating multitemporal imagery to analyze evolution of crop cycle, and integrating complementary sensing modalities (e.g., multispectral data) to improve segmentation robustness. An approach to modeling obstacles that disrupt row continuity is a promising direction for further enhancing performance in complex scenarios.

Acknowledgments

This study was supported in part by Coordenação de Aperfeiçoamento de Pessoal de Nível Superior (CAPES) – Financing Code #001, Conselho Nacional de Desenvolvimento Científico e Tecnológico (CNPq/MCTI) Nº 10/2023 - Faixa A - Grupos Emergentes (Universal 2023) – 406673/2023-3, and Fundação de Apoio à Pesquisa (FAPEG) Nº 21/2024.

References

[1] J. Shi, Y. Bai, Z. Diao, J. Zhou, X. Yao, and B. Zhang, "Row detection based navigation and guidance for agricultural robots and autonomous vehicles in row-crop fields: Methods and applications," *Agronomy*, vol. 13, no. 7, p. 1780, Jun. 2023.

[2] P. Chen, X. Ma, F. Wang, and J. Li, "A new method for crop row detection using unmanned aerial vehicle images," *Remote Sensing*, vol. 13, no. 17, p. 3526, Sep. 2021.

[3] H. Afzaal, D. Rude, A. A. Farooque, G. S. Randhawa, A. W. Schumann, and N. Krouglicof, "Improved crop row detection by employing attention-based vision transformers and convolutional neural networks with integrated depth modeling for precise spatial accuracy," *Smart Agricultural Technology*, vol. 11, p. 100934, Aug. 2025.

[4] S. Mardanisamani and M. Eramian, "Segmentation of vegetation and microplots in aerial agriculture images: A survey," *The Plant Phenome Journal*, vol. 5, no. 1, Jan. 2022.

[5] I. Vidovic, R. Cupec, and Z. Hocenski, "Crop row detection by global energy minimization," *Pattern Recognition*, vol. 55, p. 68–86, Jul. 2016.

[6] J. B. Ribeiro, R. R. da Silva, J. D. Dias, M. C. Escarpinati, and A. R. Backes, "Automated detection of sugarcane crop lines from uav images using deep learning," *Information Processing in Agriculture*, vol. 11, no. 3, p. 385–396, Sep. 2024.

[7] A. Sandhya and A. Venkataramana, "A survey on advances and insights of image analysis techniques for phenotyping in maize research: systematic review," *Discover Agriculture*, vol. 3, no. 1, p. 254, 2025.

[8] S. Zhuang, P. Wang, and B. Jiang, "Vegetation extraction in the field using multi-level features," *Biosystems Engineering*, vol. 197, p. 352–366, Sep. 2020.

[9] S. Mardanisamani and M. Eramian, "Segmentation of vegetation and microplots in aerial agriculture images: A survey," *Plant Phenome J.*, vol. 5, no. 1, Jan. 2022.

[10] Z. Luo, W. Yang, Y. Yuan, R. Gou, and X. Li, "Semantic segmentation of agricultural images: A survey," *Inf. Process. Agric.*, vol. 11, no. 2, pp. 172–186, Jun. 2024.

[11] M. Hassanein, M. Khedr, and N. El-Sheimy, "Crop row detection procedure using low-cost uav imagery system," *The International Archives of the Photogrammetry, Remote Sensing and Spatial Information Sciences*, vol. XLII-2/W13, p. 349–356, Jun. 2019.

[12] W. Winterhalter, F. V. Fleckenstein, C. Dornhege, and W. Burgard, "Crop row detection on tiny plants with the pattern hough transform," *IEEE Robotics and Automation Letters*, vol. 3, no. 4, p. 3394–3401, Oct. 2018.

[13] R. Zhao, X. Yuan, Z. Yang, and L. Zhang, "Image-based crop row detection utilizing the hough transform and DBSCAN clustering analysis," *IET Image Process.*, vol. 18, no. 5, pp. 1161–1177, Apr. 2024.

[14] M. D. Bah, A. Hafiane, and R. Canals, "CRowNet: Deep network for crop row detection in UAV images," *IEEE Access*, vol. 8, pp. 5189–5200, 2020.

[15] D. Li, B. Li, S. Kang, H. Feng, S. Long, and J. Wang, "E2CropDet: An efficient end-to-end solution to crop row detection," *Expert Syst. Appl.*, vol. 227, no. 120345, p. 120345, Oct. 2023.

[16] M. Cao, F. Tang, P. Ji, and F. Ma, "Improved real-time semantic segmentation network model for crop vision navigation line detection," *Front. Plant Sci.*, vol. 13, p. 898131, Jun. 2022.

[17] R. Doha, M. Al Hasan, S. Anwar, and V. Rajendran, "Deep learning based crop row detection with online domain adaptation," in *Proceedings of the 27th ACM SIGKDD Conference on Knowledge Discovery & Data Mining*, ser. KDD '21. New York, NY, USA: Association for Computing Machinery, 2021, p. 2773–2781.

[18] R. Storn and K. Price, "Differential evolution – a simple and efficient heuristic for global optimization over continuous spaces," *Journal of Global Optimization*, vol. 11, no. 4, p. 341–359, Dec. 1997.

[19] B. Moraes Rocha, A. Ueslei da Fonseca, H. Pedrini, and F. Soares, "Automatic detection and evaluation of sugarcane planting rows in aerial images," *Information Processing in Agriculture*, vol. 10, no. 3, p. 400–415, Sep. 2023.